LCC-0109
TESLA 2002-11
CBP Tech Note-269
November 2002

Linear Collider Collaboration Tech Notes

Alignment Stability Models for Damping Rings

Andrej Wolski
Lawrence Berkeley National Laboratory
University of California
Berkeley, CA

Winfried Decking
Deutsches Elektron Synchrotron (DESY)
Hamburg, Germany

Abstract: Linear collider damping rings are highly sensitive to magnet alignment. Emittance tuning simulations for current designs of damping rings for TESLA and NLC have given encouraging results, but depend on invasive measurements of dispersion. The frequency with which such measurements must be made is therefore an operational issue, and depends on the time stability of the alignment. In this note, we consider three effects that lead to misalignment and the need to retune the damping ring: (1) diffusive or ATL ground motion, (2) propagation of elastic ground waves leading to correlated motion of the beamline components, (3) uncorrelated motion arising from local noise sources.

LCC-0109
TESLA 2002-11
CBP Tech Note-269

Alignment Stability Models for Damping Rings

A. Wolski
LBNL

W. Decking
DESY

November 8th, 2002

Abstract

Linear collider damping rings are highly sensitive to magnet alignment. Emittance tuning simulations for current designs of damping rings for TESLA and NLC have given encouraging results, but depend on invasive measurements of dispersion. The frequency with which such measurements must be made is therefore an operational issue, and depends on the time stability of the alignment. In this note, we consider three effects that lead to misalignment and the need to retune the damping ring: (1) diffusive or ATL ground motion, (2) propagation of elastic ground waves leading to correlated motion of the beamline components, (3) uncorrelated motion arising from local noise sources.

1 Introduction

Damping rings for a future linear collider will need to operate with equilibrium vertical emittances of the order of a few picometers. Achieving such highly focused beams will depend on precise alignment of beamline components, particularly the quadrupole and sextupole magnets, and effective steering and coupling correction algorithms. Recent simulations have shown encouraging results from simple algorithms in the cases of the TESLA and NLC damping rings [1]. However, these algorithms depend on correcting the vertical dispersion to within a few hundred microns rms, and such dispersion may be generated by small movements of the quadrupoles and sextupoles.

For example, an uncorrelated quadrupole displacement of 1 μm rms will generate a closed orbit distortion of 50 μm rms in the NLC main damping ring, and an uncorrelated beam offset of 50 μm rms in the sextupoles will generate 3 mm rms vertical dispersion, which in turn will generate 4 pm vertical emittance (even neglecting the effects of betatron coupling). The specified upper limit for the vertical emittance in the NLC is 3.4 pm. Although these statements would seem to imply an unrealistic requirement for vertical alignment of the quadrupoles to better than 1 μm, one needs to exercise some caution in their interpretation. Typically, the closed orbit distortion is dominated by the principal betatron modes, and the beam offsets in the sextupoles are therefore correlated. The vertical dispersion can be less sensitive to correlated beam offsets than to correlated offsets. Similarly, quadrupole motion on intermediate and long timescales (greater than the order of 1 second) are expected to be highly correlated. In the extreme case, a low frequency, long wavelength ground wave will move the ring as a whole, and the emittance will not be significantly affected.

A simple assumption of uncorrelated component motion is likely to be significantly pessimistic, and it is important to apply realistic (or at least semi-realistic) models of component motion to the damping rings, to determine the frequency with which emittance tuning must be performed. Orbit correction on frequency scales of the order 1 Hz is possible, but dispersion correction requires invasive measurements, and the frequency with these measurements are required has a direct impact on operational efficiency.

Besides emittance growth, one needs to consider orbit jitter arising from quadrupole motion. Without correction, a beam extracted from the damping ring with significant transverse offset can be expected to perform betatron oscillations through to the interaction point. This has undesirable consequences, for example emittance growth from wake fields in the main linac cavities. Although corrections can be applied, it is important to understand how large the jitter from the damping rings might be.

Alignment stability is also an important issue for other parts of a linear collider, including the main linac, beam delivery system and final focus. Significant effort has gone into studies of environments in which such systems may be expected to operate, with the aim of collecting and understanding data, and developing models which may be applied to designs in development. It seems sensible to apply the same models to the damping rings as are used for other systems in a linear collider: this is the aim of the present note. Relevant data do exist for existing storage rings; orbit stability is an important issue for synchrotron light sources, for example. It is beyond our present scope, but we recommend that a comprehensive survey of existing data be carried out in the context of the requirements for linear collider damping rings.

We consider here three separate (though not entirely distinct) effects leading to changes in alignment of the damping ring components. These are:

- diffusive (ATL) ground motion;
- propagation of elastic ground waves;
- vibration from local noise sources.

The first two effects lead to component motion correlated in time and space. The vibration from local sources is assumed to be uncorrelated.

2 Diffusive Ground Motion

2.1 ATL for 2-Dimensional Geometries

We use a simplified model of diffusive ground motion, which may be expressed in the formula (the ATL model):

$$\left\langle \left(Y_i - Y_j\right)^2 \right\rangle = ATL_{ij} \qquad \textbf{(1)}$$

where Y_i is the vertical position of the i^{th} beamline component relative to some (conceptual) fixed reference point, T is the time after initial (perfect) alignment, L_{ij} is the horizontal distance between components i and j. A is a constant characteristic of the site on which the accelerator is built: "quieter" or "more stable" sites have a lower value of A.

It is straightforward to apply the ATL model to a linear beamline. Starting at one end, one simply takes consecutive components, and vertically misaligns each component relative to the previous one, by a random value with variance given by the right hand side of (1). This procedure automatically produces a "random walk" with the correct correlation between any two components in the beamline.

The same procedure cannot be directly applied to a storage ring. For example, one result would be a correlation in the misalignment of the selected start and end points characterized by the circumference of the lattice, rather than the real distance between these points, which will generally be close to zero (or a few meters, rather than some hundreds or thousands of meters). However, it is possible to generalize this model [2]. First, we choose a fixed reference point j=0, and write:

$$\left\langle Y_i^2 \right\rangle = ATL_{i0}$$

from which it follows that:

$$\begin{aligned} \left\langle Y_i Y_j \right\rangle &= AT\,\tfrac{1}{2}\left(L_{i0} + L_{j0} - L_{ij}\right) \\ &= ATM_{ij} \end{aligned}$$

which defines the matrix **M** with elements M_{ij}. We can write this latter equation in terms of the outer product of the vector **Y** (with elements Y_i) with itself:

$$\left\langle \mathbf{Y} \cdot \mathbf{Y}^{\mathrm{T}} \right\rangle = AT\mathbf{M}$$

Since **M** is symmetric, it can be diagonalized by a unitary matrix $\mathbf{\Lambda}$:

$$\begin{aligned} \tilde{\mathbf{M}} &= \mathbf{\Lambda} \cdot \mathbf{M} \cdot \mathbf{\Lambda}^{\mathrm{T}} \\ \tilde{M}_{ij} &= \lambda_i \delta_{ij} \end{aligned}$$

where λ_i is the i^{th} eigenvalue of **M**, and δ_{ij} is the Kronecker delta symbol. $\mathbf{\Lambda}$ is of course constructed from the eigenvectors of **M**. We define the vector **V**:

$$\mathbf{V} = \mathbf{\Lambda} \cdot \mathbf{Y}$$

the elements of which clearly satisfy:

$$\left\langle V_i^2 \right\rangle = AT\lambda_i \qquad \textbf{(2)}$$

Equation (2) is all we need to apply the ATL diffusive ground motion model[1] to a general system of points on a plane (of course, the linear geometry is a special case of the generalized model). From the symmetric matrix of horizontal distances between the components and a chosen fixed reference point, we construct the matrix **M**, and find its eigensystem. We then generate a set of values with variances given by the eigenvalues of **M**, and transform these values using the eigenvectors to find the appropriate vertical displacements of the components.

[1] Although it is still ATL, we might call this generalized expression the "AT Lambda" model!

The matrix **M** has N^2 components, where N is the number of components in the lattice. For a large storage ring, N can be many hundreds, or even thousands, and we are required to find the eigensystem of a large matrix. Fortunately, efficient numerical algorithms exist to perform this task for a symmetric matrix [3], and we only need to do this once for any given geometry.

2.2 Application to TESLA and NLC Damping Rings

Emittance tuning algorithms for the TESLA and NLC damping rings have been described previously [1]. In both cases, the algorithms employ correction of the vertical orbit and dispersion. Orbit correction is straightforward, and can be applied with a frequency of 1 Hz or greater. We assume, however, that the dispersion correction requires an invasive dispersion measurement, the frequency of which will directly affect the operational efficiency of the collider. For some period of time, orbit correction alone will be sufficient to maintain the required emittance, but eventually, a dispersion correction will be needed. Using the diffusive ground motion model described above, we can estimate the rate of emittance growth, assuming orbit correction every second or few seconds. The results will indicate how frequently dispersion correction is required.

Our simulations were carried out using MERLIN. Starting from "perfect" lattices, we applied 100 μm rms rotation on the quadrupoles, followed by 50 hours of ATL ground motion to misalign the quadrupoles and sextupoles. We then applied a full emittance tuning, involving orbit and dispersion correction. For each of 20 different random seeds for the ground motion, we then studied the emittance growth over 24 hours.

Three different parameter sets are in common use for describing ground motion for linear collider studies [4]; these are referred to as Ground Motion Models A ("quiet" site), B ("intermediate" site) and C ("noisy" site). The corresponding values for the diffusion parameter A are given in Table 1.

Table 1

ATL parameters for three standard ground motion models.

Ground Motion Model	ATL Parameter A / m^2/m/s
A	10^{-19}
B	5×10^{-19}
C	10^{-17}

Results are shown in Figure 1 for NLC, and in Figure 2 for TESLA. For both machines, reasonable requirements on the orbit correction give good emittance stability, with indications that dispersion tuning may not be needed more than once every few days, even on a "noisy" site. Although this result may be rather optimistic, there appears to be a comfortable margin in the alignment stability of both rings under the influence of ATL ground motion.

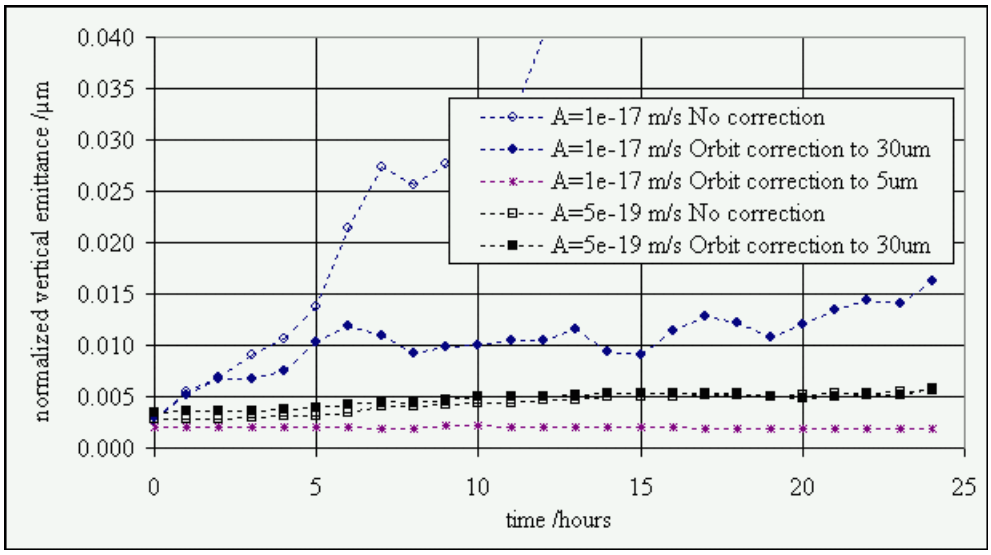

Figure 1

Stability of the vertical emittance in the NLC main damping rings, under the effects of ATL ground motion. Results are shown only for ground motion models B and C. The specified vertical emittance limit is 0.013 µm rad.

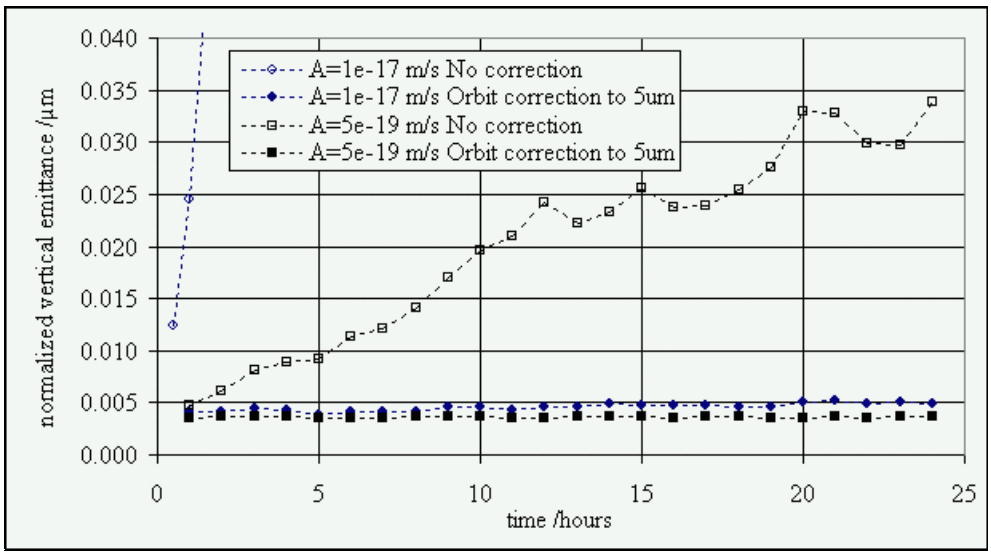

Figure 2

Stability of the vertical emittance in the TESLA damping rings, under the effects of ATL ground motion. Results are shown only for ground motion models B and C. The specified vertical emittance limit is 0.014 µm rad.

3 Elastic Ground Waves

3.1 A model

We shall see that the power contained in the region of the ground motion spectrum corresponding to the length of a bunch train is small enough that transverse jitter along a bunch train is negligible. In this section, therefore, we are concerned with the pulse-to-pulse stability of the extracted beam. Our analysis will be based on the response of the

closed orbit to the quadrupole motion, so we should properly consider only frequencies that are low compared to the damping rate. Since higher frequencies will also make some contribution to the orbit jitter, however, we shall make the approximation that the damping time is effectively zero. In practice, this will overestimate the jitter, though the power in frequencies over 100 Hz is generally small enough that motion above this frequency makes only a small contribution to the jitter.

The change in the closed orbit at a location s in the ring resulting from changes in the quadrupole alignments can be written:

$$\Delta y(s) = \frac{\sqrt{\beta_y(s)}}{2\sin(\pi\nu_y)} \sum_i \sqrt{\beta_y(s_i)}(k_1 l)_i Y_i \cos\left(\pi\nu_y + \left|\mu_y(s) - \mu_y(s_i)\right|\right)$$

where the summation is over all quadrupoles in the lattice. Y_i is the change in vertical alignment of the i^{th} quadrupole, and all other symbols have the usual meanings. Thus, the mean square orbit change over a number of sets of quadrupole displacements and normalized to the beam size is:

$$\frac{\left\langle \Delta y(s)^2 \right\rangle}{\sigma_y^2} = \frac{\mathrm{Tr}(\mathbf{G}\cdot\mathbf{F})}{4\varepsilon_y \sin^2(\pi\nu_y)} \qquad \textbf{(3)}$$

where **G** and **F** are matrices with elements:

$$G_{ij} = \sqrt{\beta_y(s_i)\beta_y(s_j)}(k_1 l)_i (k_1 l)_j \cos\left(\pi\nu_y + \left|\mu_y(s) - \mu_y(s_i)\right|\right)\cos\left(\pi\nu_y + \left|\mu_y(s) - \mu_y(s_j)\right|\right)$$

$$F_{ij} = \left\langle Y_i Y_j \right\rangle$$

Note that **G** is characteristic of the lattice (and a function of location in the lattice), and **F** is characteristic of the ground motion. For uncorrelated motion, **F** is diagonal. For ground waves with wavelengths much longer than the dimensions of the ring, all the components of **F** are roughly equal; in this case the orbit is not significantly distorted, but moves "coherently" with the quadrupoles. In our model, we introduce a low-frequency cut-off in the power spectrum of ground motion, such that we retain motion that is correlated only over distances up to the betatron wavelength. We discuss this further below.

Note also that the geometry of the problem enters through the matrix **G**. In our treatment of ATL motion, we constructed a model that allowed us to put misalignments on magnets with the correct correlation over a closed lattice. For the present study of ground waves, we require only the form of this correlation between different points on the lattice; it makes no difference whether the lattice has a linear or circular geometry.

Our treatment of the ground motion is based on the work of Napoli and Seryi [5]. Their model was developed for the study of ground motion effects in (normal conducting) linacs, and there are significant differences between linacs and storage rings that mean the model might not be entirely appropriate. These differences lie in the components of the lattice, as well as in the location and overall construction. For example, the strong

focusing magnets in a storage ring might be physically heavier than those in a linac, and mounted on large girders with lower resonant frequencies. It is possible that the damping rings might be at a shallower depth than the main linac, or that the magnets are hung from the roof of the tunnel. All these issues can affect the validity of a particular model; this is an area where further research could be done, and for the present we shall apply the same models to the damping rings as are used for the linacs.

In terms of the two-dimensional power spectrum, we can write:

$$F_{ij} = \int_{-\infty}^{\infty}\frac{\mathrm{d}\omega}{2\pi}\int_{-\infty}^{\infty}\frac{\mathrm{d}k}{2\pi}P(\omega,k)\cos\left(kL_{ij}\right) \approx 2\int_{0}^{\infty}\frac{\mathrm{d}\omega}{2\pi}\int_{0}^{\infty}\frac{\mathrm{d}k}{2\pi}P(\omega,k)\cos\left(kL_{ij}\right)$$

where in the approximation, we have assumed that $P(\omega,k)$ is zero for $\omega<0$, and is an even function of k. Following [5], and introducing an approximation for the function U, we write:

$$\begin{aligned} P(\omega,k) &= D(\omega)U(\omega,k) \\ D(\omega) &= \frac{a_\mu}{1+\left[d_\mu\dfrac{(\omega-\omega_\mu)}{\omega_\mu}\right]^4} \\ U(\omega,k) &= \frac{2}{\sqrt{\dfrac{\omega^2}{v(\omega)^2}-k^2}} \approx 2\frac{v(\omega)}{\omega} \qquad |k|<\frac{\omega}{v(\omega)} \end{aligned} \tag{4}$$

where the model is specified by the parameters a_μ, d_μ, ω_μ and the velocity $v(\omega)$. A spectrum is constructed from "resonance peaks" labeled by the index μ. We consistently use:

$$v(\omega)[\mathrm{m/s}] = 450 + 1900\exp\left(-\omega[\mathrm{s}^{-1}]/4\pi\right)$$

Note that the power content of the motion falls with the fourth power of the frequency.

We consider first the case of a ground motion spectrum consisting of a single resonance peak, and then consider the more general case of several peaks.

3.1.1 Ground motion spectrum with a single resonance peak

Introducing the low frequency cut-off ω_c mentioned above, we make the approximation:

$$D(\omega) \approx a_\mu\left(\frac{\omega_\mu}{d_\mu}\right)^4\frac{1}{\omega^4} \qquad \omega > \omega_c >> \omega_\mu \tag{5}$$

and thus:

$$F_{ij} \approx 4\frac{a_\mu\omega_\mu^4}{d_\mu^4}\int_{\omega_c}^{\infty}\frac{\sin\left(\omega L_{ij}/v_c\right)}{\omega^5 L_{ij}/v_c}\mathrm{d}\omega$$

where $v_c = v(\omega_c)$. One advantage of this approximation is that it is convenient for computations, to write the components of the correlation matrix in terms of a special function (the generalized hypergeometric function ${}_1F_2$):

$$F_{ij} \approx \frac{4a_\mu \omega_\mu^4}{3d_\mu^4 \omega_c^3} \tilde{F}\left(\tfrac{1}{2} k_c L_{ij}\right)$$

where

$$k_c = \frac{\omega_c}{v(\omega_c)}$$

$$\tilde{F}(x) = {}_1F_2\left(-\tfrac{3}{2}; -\tfrac{1}{2}, \tfrac{3}{2}; -x^2\right) + \frac{\pi}{2} x^3$$

It turns out that the approximations may be improved for frequencies approaching the resonant frequency ω_μ, by introducing a "form factor":

$$F_{ij} \approx \frac{4a_\mu \omega_\mu^4}{3d_\mu^4 \omega_c^3} \tilde{F}\left(\tfrac{1}{2} k_c L_{ij}\right) f\left(\frac{\omega_\mu}{\omega_c}\right)$$

where

$$f(x) = 12x^2 + 2.6x + 1$$

Note that the distance between elements appears only in the function $\tilde{F}(x)$. This function is useful for understanding the correlation in the motion for different elements. A plot of $\tilde{F}(x)$ is shown in Figure 3.

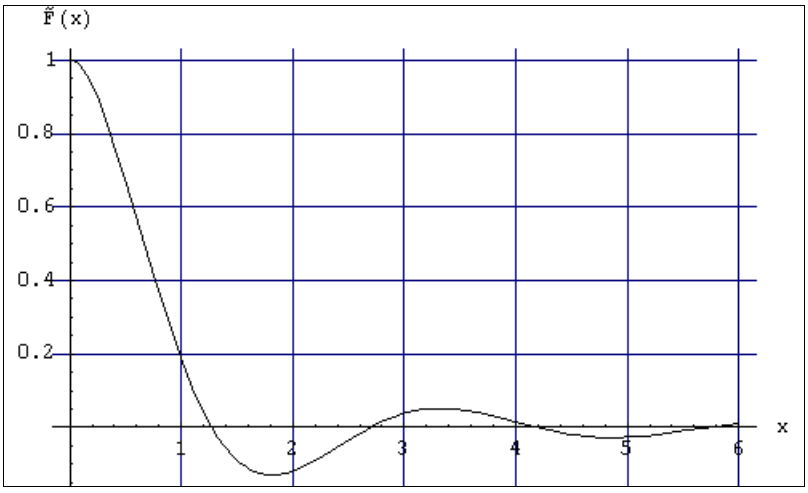

Figure 3
Correlation function $\tilde{F}(x)$.

We can check the validity of the approximation (5) by considering the special case of the ground motion model C [4], referred to in Section 2.2 above. We shall find that appropriate cut-off frequencies for the damping rings are $\omega_c/2\pi$ = 5 Hz in the case of

TESLA, and $\omega_c/2\pi$ = 10 Hz for NLC. Ground motion model C has a peak (μ = 2) at 2.5 Hz. Comparisons of the correlation function F_{ij} for this peak using the approximation in equation (5) and the more exact expression in equation (4) are shown in Figure 4 ($\omega_c/2\pi$ = 10 Hz) and Figure 5 ($\omega_c/2\pi$ = 5 Hz). The agreement is excellent for the 10 Hz cut-off, and reasonably good for the 5 Hz cut-off.

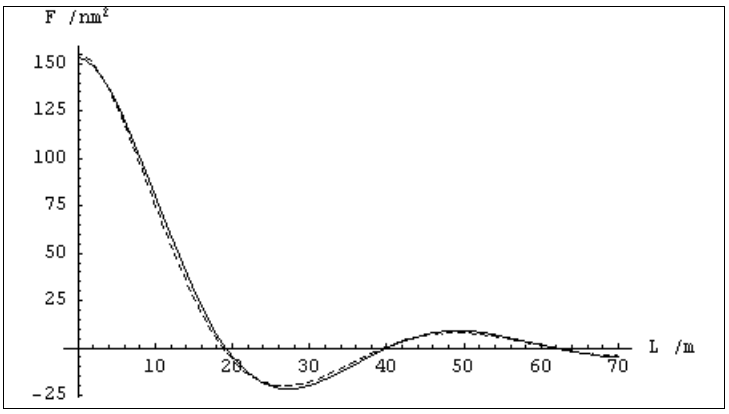

Figure 4

Comparison of the correlation matrix in two approximations (solid line for equation 3, and broken line for the approximation of equation 4), for the ground motion model C, μ = 2, and $\omega_c/2\pi$ = 10 Hz.

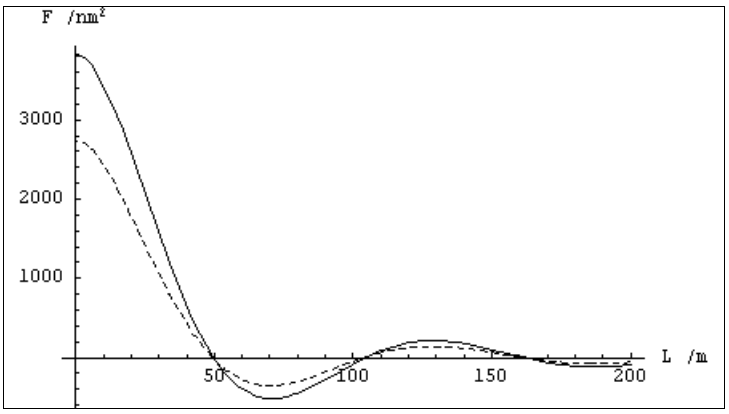

Figure 5

Comparison of the correlation matrix in two approximations (solid line for equation 3, and broken line for equation 4), for the ground motion model C, μ= 2, and $\omega_c/2\pi$ = 5 Hz.

The three ground motion models also include resonant peaks at frequencies larger than the appropriate cut-off frequencies. However, the amplitudes of these peaks are such that they make negligible contribution to the orbit jitter. The reason for this is that the magnet motion arising from these high frequency peaks is effectively uncorrelated (for magnets more than about 1 m apart), and with a magnitude of the order of a nanometer or less (observe the scales in Figure 4 and Figure 5, for the "middle frequency" peaks that have a

much larger amplitude). We expect other sources of noise to contribute to uncorrelated magnet motion of the order of tens of nanometers.

3.1.2 Full ground motion spectra

The power spectra for the standard ground motion models are shown in Figure 6. In the approximation (5), we replace these with spectra given by:

$$\begin{aligned} D(\omega) &= \frac{P_0}{\omega^4} \qquad \omega > \omega_c \\ &= 0 \qquad \omega < \omega_c \end{aligned} \tag{6}$$

where P_0 is chosen to fit the spectrum. In fact, a good fit is given by:

$$P_0 = \sum_{\mu} a_{\mu} \left(\frac{\omega_{\mu}}{d_{\mu}} \right)^4 \tag{7}$$

where we sum over all frequency peaks. The resulting fits are shown in Figure 7.

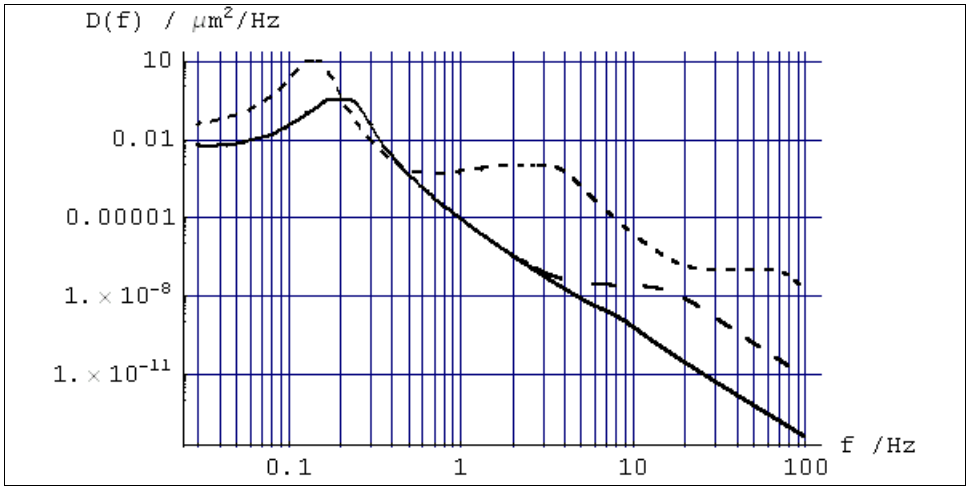

Figure 6

Power spectrum for ground motion models A (solid line), B (dashed line) and C (dotted line).

3.1.3 Deciding the low-frequency cut-off

Selecting a high value for the cut-off frequency ω_c risks excluding a significant amount of power from the spectrum. On the other hand, the orbit jitter induced by very low frequency motion (which has a relatively large amplitude) is suppressed by the correlation in the motion between different magnets. The scale is set by the betatron wavelength; an appropriate value for the cut-off frequency is found from the condition that the waves below this frequency have wavelengths longer than the betatron wavelength:

$$k_c \approx \frac{1}{\beta_y}$$

This is consistent with the correlation function shown in Figure 3, where it appears that the correlation length for the magnet motion is given roughly by:

$$L_{ij} \approx \frac{1}{k_c}$$

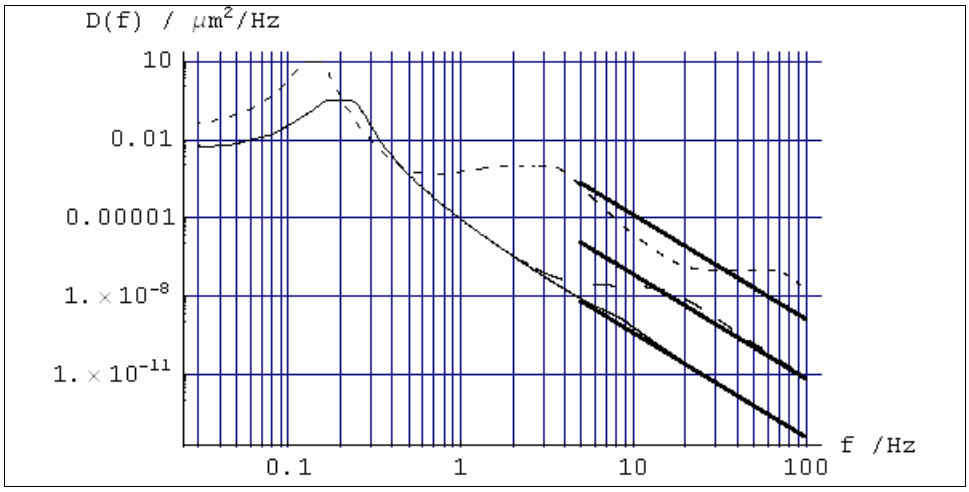

Figure 7

Approximations to the ground motion spectra (bold lines), using (5) and (6) and $\omega_c/2\pi$ = 5 Hz.

This gives us a rough guide in setting the cut-off frequency. As a consistency check, we can look at the mean magnet displacement compared to the beam displacement. If the ratio of these two values is significantly large, this indicates coherent motion of the lattice, and the frequency cut-off has been set too low. Since

$$\left\langle \bar{Y}^2 \right\rangle = \frac{1}{N^2} \sum_{ij} \left\langle Y_i Y_j \right\rangle = \frac{1}{N^2} \sum_{ij} F_{ij}$$

where $\bar{Y}$ is the mean magnet displacement, and

$$\left\langle \overline{\Delta y^2} \right\rangle = \frac{\overline{\beta_y} \mathrm{Tr}\left(\mathbf{G} \cdot \mathbf{F}\right)}{4 \sin^2\left(\pi \nu_y\right)}$$

we can readily calculate the required ratio:

$$r = \sqrt{\frac{\left\langle \bar{Y}^2 \right\rangle}{\left\langle \overline{\Delta y^2} \right\rangle}}$$

Note that we use the square of the mean magnet displacement, and the mean of the squared orbit distortion; this is appropriate to test for coherent motion of the lattice. Our consistency condition for the cut-off frequency is that r should be small (i.e. much less than one).

3.2 Application to TESLA and NLC Damping Rings

What are the appropriate cut-off frequencies for the damping rings? For NLC, we take an average value $\beta_y \approx 7$ m, which gives $\omega_c/2\pi \approx 10$ Hz. For TESLA, the beta functions are rather larger in the straights; however taking too small a value for the cut-off violates the assumption that the important frequency range is much larger than the resonant peaks in the ground motion spectrum. We compromise, and take $\omega_c/2\pi \approx 5$ Hz, which corresponds to a beta function of $\beta_y \approx 20$ m. It turns out that for each case (TESLA and NLC), the value of *r* (ratio of the mean magnet motion to the mean beam motion) is about 0.015.

We are now ready to calculate the rms beam jitter as a fraction of the beam size. In Table 2 we show the jitter that may be expected using the approximations (6) and (7) to each of the ground-motion models. The correlation function is calculated from:

$$F_{ij} = \frac{4P_0}{3\omega_c^3}\tilde{F}\left(\tfrac{1}{2}k_c L_{ij}\right)$$

and we then use (3) to calculate the jitter.

Table 2

Predicted beam jitter from correlated ground motion.

Model	Amplitude P_0 /μm^{2}s^{-3}	TESLA		NLC	
		$\omega_c/2\pi$	$\sqrt{\langle \Delta y^2 \rangle}/\sigma_y$	$\omega_c/2\pi$	$\sqrt{\langle \Delta y^2 \rangle}/\sigma_y$
A	0.0062	5 Hz	0.0012	10 Hz	0.00054
B	1.1	5 Hz	0.016	10 Hz	0.0071
C	200	5 Hz	0.217	10 Hz	0.099

Our simplified model gives the approximate scaling:

$$\frac{\langle y^2 \rangle}{\sigma_y^2} \propto P_0 \qquad \textbf{(8)}$$

The jitter is negligible in models A and B, and still within tolerable limits in model C. Results of earlier studies were reported in the NLC ZDR [6]; these studies considered an earlier design of the damping ring, though one that was not too dissimilar to the present design. For P_0=0.0016, it was found that $\sqrt{\langle \Delta y^2 \rangle}/\sigma_y \approx 2.8\times10^{-5}$. Using the simple scaling (8), this level of ground motion for the present design would give a value of 2.7×10^{-4}. The apparent greater sensitivity of the present lattice by an order of magnitude might be partially accounted for by the stronger focusing (lower natural emittance with fewer arc cells at the same energy), and the non-optimal vertical tune, which is significantly further from the half-integer compared to the ZDR design. However, our treatment is also rather pessimistic in comparison to the ZDR approach. Our approach roughly relates to that in the ZDR, if one replaces the lattice response function by a step

function, with the step at the cut-off frequency[2]. Following the ZDR, we would have placed the cut-off at around $\omega_c/2\pi \approx 50$ Hz, rather than the 10 Hz we have actually used. This would reduce the jitter by nearly a factor of 5, and the remaining factor 2 is accounted for by changes in the lattice.

3.3 Uncorrelated Motion

The effects of uncorrelated motion may be extracted from the previous treatment as a special case, with a diagonal correlation matrix **F**; the elements are just the mean square displacements of the quadrupoles. For both NLC and TESLA, we find that quadrupole motion of approximately 80 nm rms will give an orbit jitter equal to the vertical beam size. Such motion can easily occur if the magnet supports and cooling systems etc. are not properly designed, but with care, it should be possible to keep the vibration well below this level. We note that it may be possible to use a fast orbit feedback system to keep the orbit stable at the extraction point, and thus ease the tolerances on the magnet motion (this applies for both correlated and uncorrelated motion).

Again comparing to the NLC ZDR for comparison with the earlier NLC damping ring design, we find that the present design has a greater sensitivity, though by a factor of 2 rather than an order of magnitude (as was the case for correlated motion from ground waves). This factor can be accounted for by changes in the lattice.

4 Conclusions

Models exist for describing ground motion effects on linear colliders. It is possible to apply these models to the damping rings, providing a description consistent with other parts of the machine. The models include both diffusive (ATL) ground motion, and (with some approximations) the propagation of elastic waves.

- Simulations suggest that orbit correction will be sufficient in both the TESLA and NLC damping rings to maintain the required vertical emittance under the effects of ATL ground motion, over timescales of the order of several days. This applies to each of the three parameter sets, corresponding to sites of different activity.
- Elastic waves can lead to jitter in the extracted beam. The noisiest site considered here could give significant jitter for both TESLA and NLC, but still within the specified limit.
- Sources of noise leading to uncorrelated magnet vibrations of 80 nm rms will give vertical jitter comparable to the beam size; attention will need to be paid to the design of mechanical systems to ensure that the vibrations remain well below this level.
- We have applied the ground motion models developed for studies of the main linacs to the damping rings. Differences between the two systems mean that this might not be entirely appropriate, but at the present time represents the best approximation we can make.

[2] This is not completely true, since we have our own response function in the matrix **F**.

In connection with the last of these points, we emphasize the need for a study of the experience of existing machines. As we mentioned above, orbit stability is an issue for third generation light sources, which are similar in many respects to the damping rings.

Acknowledgement

We are grateful to Andrei Seryi for making helpful comments and suggestions.

References

[1] W. Decking and A. Wolski, "Comparison of Emittance Tuning in the NLC and TESLA Damping Rings", August 2002.
[2] Thanks to Nick Walker for proposing and explaining this method.
[3] In the simulation code MERLIN, the Householder algorithm is used to reduce the matrix to tridiagonal form, and a QL algorithm then applied to find the eigensystem. Implementations are given and explained in W.H. Press, S.A. Teukolsky, W.T. Vetterling, B.P. Flannery, "Numerical Recipes in C", Second Edition 1992, Cambridge University Press.
[4] A. Seryi, http://www.slac.stanford.edu/~seryi/gm/model/
[5] A. Seryi, O. Napoly, Phys.Rev.E 53, 5323 (1996).
[6] The NLC Design Group, "Zeroth-Order Design Report for the Next Linear Collider", SLAC-474, 1996, pp.223-225.